

## CME modeling at the CPA of KU Leuven

E. Chané & S. Poedts & B. van der Holst & C. Jacobs &  
 G. Dubey & D. Kimpe

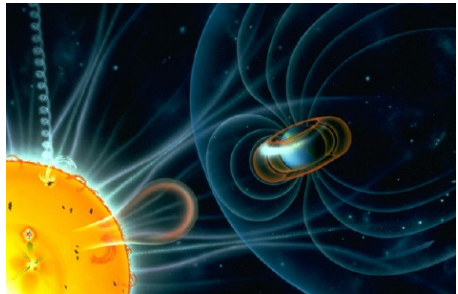
Centre for Plasma Astrophysics  
 K.U.Leuven

COST724 workshop, Athens, 13 October, 2005

## Motivation : space weather

### USA NSWP Strategic Plan:

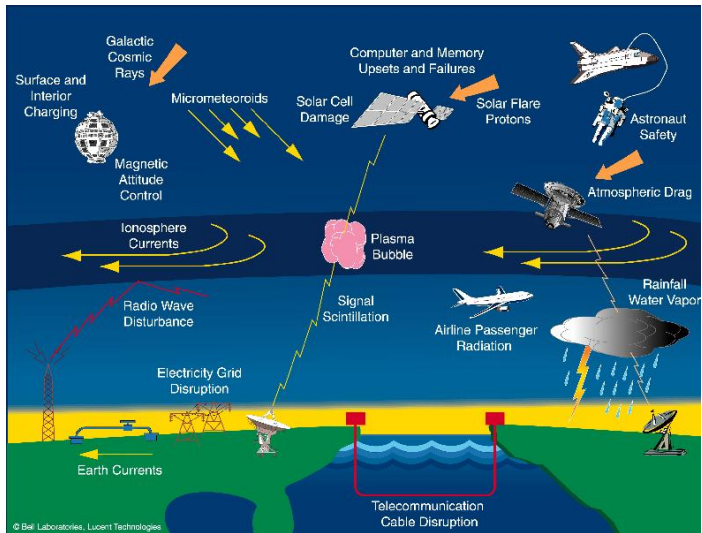
*"Space Weather refers to conditions on the sun and in the solar wind, magnetosphere, ionosphere, and thermosphere that can influence the performance and reliability of space-borne and ground-based technological systems and can endanger human life or health."*



### *Space weather =*

time-dependent disturbances of the Earth's magnetosphere driven by solar activity in a wide range of spatial and temporal scales

# Space weather effects



## Space weather : drivers

- drivers are of solar origin:, viz. transient phenomena superposed on the solar wind:
  - CMEs (most prominent)
  - eruptive flares
  - Solar Energetic Particle events
  - ...
- basic physical mechanisms not fully understood
- 2 out of 3 predictions are **WRONG !**

### *CMEs :*

- typ. 400 km/s,  $10^{12} - 10^{13}$  kg!
- $E = 10^{24} - 10^{25}$  Joule
- known since 30 yrs only!
- **they play a crucial role in SW!**

## Motivation

Construction of **numerical models** for the **solar wind** and **CME initiation and evolution** in order to improve prediction of space weather.

## Motivation

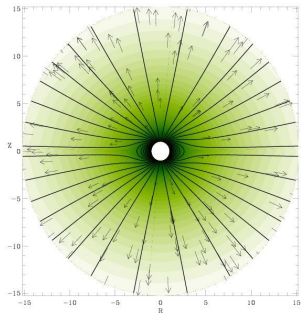
Construction of **numerical models** for the **solar wind** and **CME initiation and evolution** in order to improve prediction of space weather.

## Comparative studies

Study **the effect of the background solar wind and CME parameters** on the **initiation** and **evolution** of IP CMEs and CME shocks.

- in an **objective way**, i.e. with the same numerical code, grid resolution (numerical dissipation), numerical technique, BCs & ICs, etc.
- in order to **quantify the effect of the background wind and initiation parameters** on the CME speed, the direction, density, magnetic field etc.

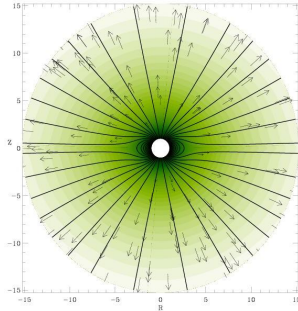
## Solar wind models



### *Polytropic Wind*

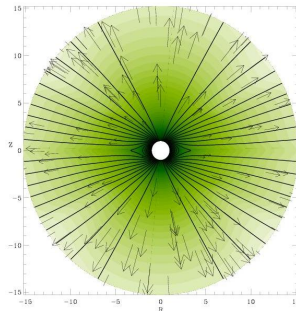
Color: density (log-scale), black lines:  
 magnetic field lines, arrows: velocity

## Solar wind models



*Polytropic Wind*

Color: density (log-scale), black lines:  
 magnetic field lines, arrows: velocity



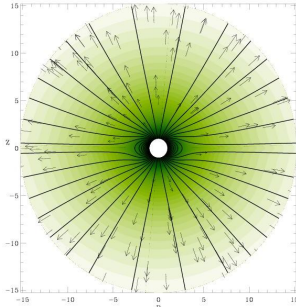
*'Manchester' wind*

Extra heating source term:

$$Q = \rho q_0 e^{-\frac{(r-r_0)^2}{\sigma^2}} \left( T_0 - \gamma \frac{P}{\rho} \right)$$

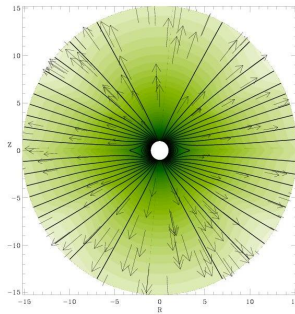


## Solar wind models



### *Polytypic Wind*

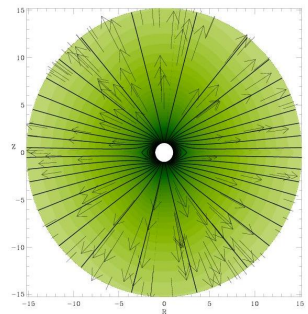
Color: density (log-scale), black lines:  
 magnetic field lines, arrows: velocity



### *'Manchester' wind*

Extra heating source term:

$$Q = \rho q_0 e^{-\frac{(r-r_0)^2}{\sigma^2}} \left( T_0 - \gamma \frac{P}{\rho} \right)$$



### *Polytypic Wind with Alfvén Waves*

Has additional Alfvén wave pressure  
 gradient.

## Wind characteristics at $30R_{\odot}$

	Model 1	Model 2	Model 3
<i>Density</i> [ $m^{-3}$ ]			
Pole	$5.6 \times 10^8$	$1.02 \times 10^9$	$3.08 \times 10^9$
Equator	$7.27 \times 10^8$	$1.83 \times 10^9$	$2.87 \times 10^9$
Ratio	0.77	0.56	1.07
<i>Velocity</i> [km/s]			
Pole	323	727	675
Equator	293	358	374
Ratio	<b>1.1</b>	<b>2.03</b>	<b>1.8</b>
<i>Temperature</i> [K]			
Pole	$0.82 \times 10^6$	$1.13 \times 10^6$	$0.89 \times 10^6$
Equator	$0.83 \times 10^6$	$0.29 \times 10^6$	$0.89 \times 10^6$
Ratio	0.99	3.87	1.0
<i>Magnetic field</i> [G]			
Pole	$6.04 \times 10^{-4}$	$3.7 \times 10^{-4}$	$3.9 \times 10^{-4}$
Equator	$6.1 \times 10^{-5}$	$1.2 \times 10^{-4}$	$2.0 \times 10^{-4}$
Ratio	9.89	3.06	1.95

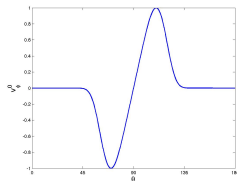
## CME initiation: Shearing

Add extra azimuthal velocity  $v_{\phi}^0$  at the solar surface to shear the footpoints of the magnetic field.

magnetic field lines

$$v_{\phi}^0 = v_0(t)\Theta e^{(1-\Theta^4)/4}$$

$$\text{with } \Theta = \frac{\theta - \pi/2}{\Delta\theta_m}$$



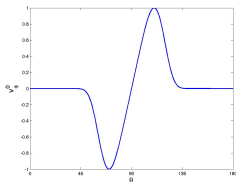
Background wind: *Model 1*, maximum shear velocity: *6 km/s*.

## CME initiation: Shearing

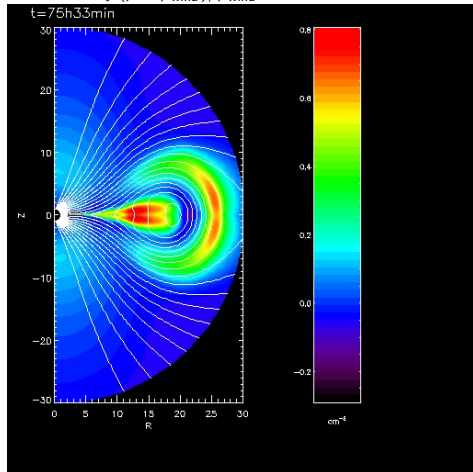
Add extra azimuthal velocity  $v_{\phi}^0$  at the solar surface to shear the footpoints of the magnetic field.

$$v_{\phi}^0 = v_0(t)\Theta e^{(1-\Theta^4)/4}$$

$$\text{with } \Theta = \frac{\theta - \pi/2}{\Delta\theta_m}$$



relative density  $(\rho - \rho_{wind})/\rho_{wind}$

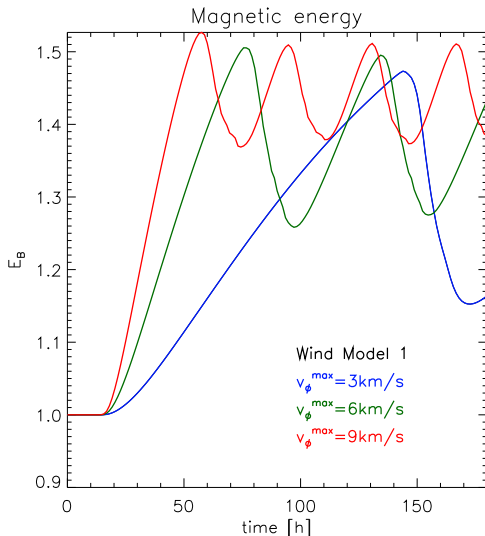


Background wind: **Model 1**, maximum shear velocity: **6 km/s**.

# CME initiation: Shearing - parameter studies

## Shearing rate affects

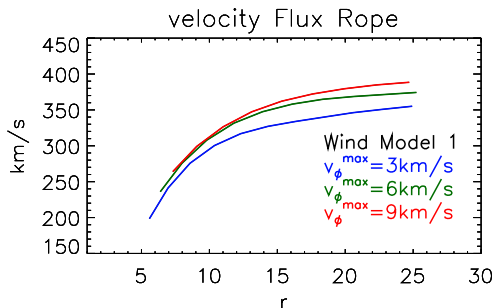
- $\Delta t$  to reach instability
- instability threshold in terms of energy
- amount of energy released
- velocity/acceleration of flux rope
- ...



## CME initiation: Shearing - parameter studies

### Shearing rate affects

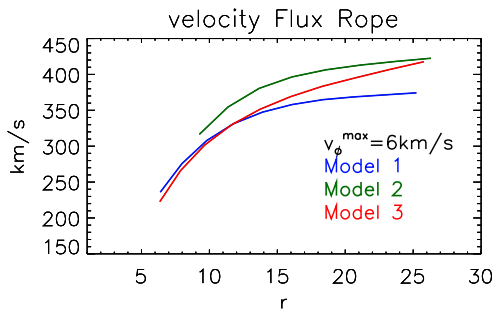
- $\Delta t$  to reach instability
- instability threshold in terms of energy
- amount of energy released
- **velocity/acceleration of flux rope**
- ...



## CME initiation: Shearing - parameter studies

### Background wind affects

- $\Delta t$  to reach instability
- instability threshold in terms of energy
- amount of energy released
- **velocity/acceleration of flux rope**
- ...

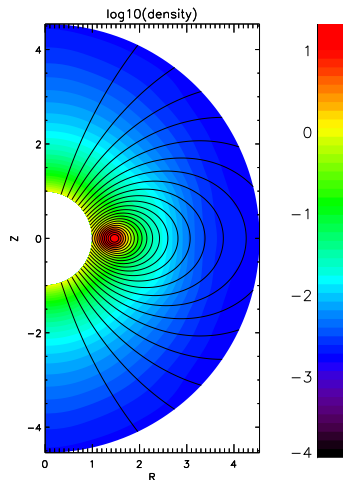


# CME initiation: flux emergence / cancellation

## Initial model

- cf. Chen & Shibata (2000)
  - + **physics** : MHD (incl. gravity)
  - + **geometry** : 2D (axisymmetric)
  - + dipole field
- OR
- + **solar wind** ⇒

$$\vec{B}_0 = \vec{B}_{LC} + \vec{B}_{IC} + \vec{B}_{BG}$$



Initial  $\rho$  and  $\vec{B}$  (relaxed until  $t = 32$ )

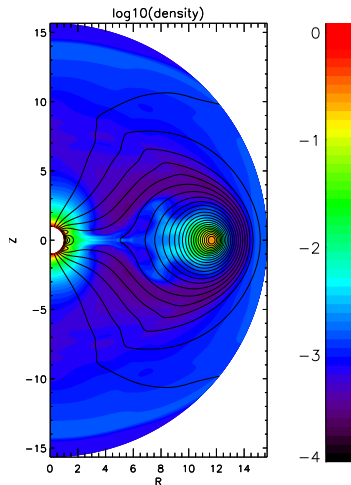
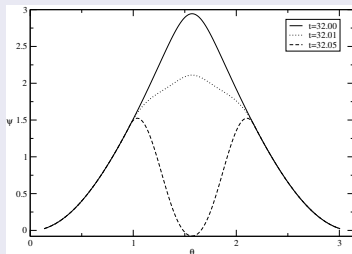


# CME initiation: flux emergence / cancellation

## Addition of flux

cf. Forbes & Priest ('84), Chen & Shibata ('00)

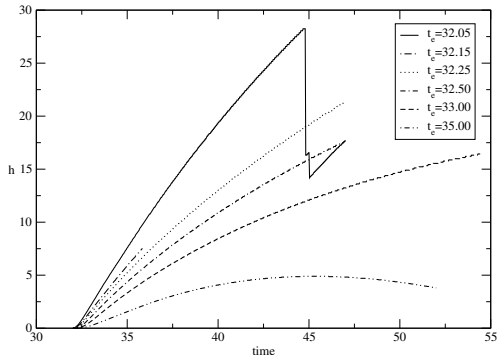
- at lower boundary ( $r = 1R_{\odot}$ )
- in region  $\frac{\pi}{2} - 0.6 \leq \theta \leq \frac{\pi}{2} + 0.6$
- BC:  $A_{\varphi} = A_{\varphi}(t_0) + c_e A_{\varphi}^+ \frac{t - t_0}{t_e - t_0}$



## CME initiation: flux emergence / cancellation

### Parameter study : $t_e$

- fixed amount of flux:  
 $2\pi c_e \psi_0 \approx -6.6 \times 10^{20}$  Mx in Northern hemisphere
- vary *flux emergence rate*, i.e.  $2\pi c_e \psi_0 / \Delta t$  from  $-3 \times 10^{18}$  to  $-5 \times 10^{16}$  Mx/s

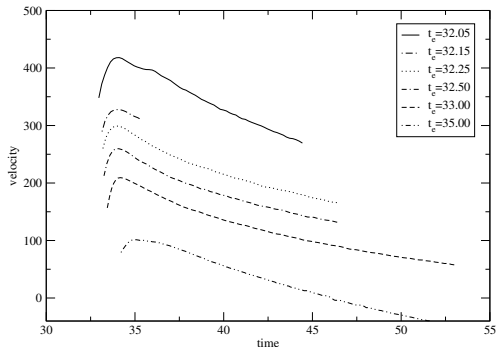


Height - time plot for difference flux emergence rates

## CME initiation: flux emergence / cancellation

### Parameter study : $t_e$

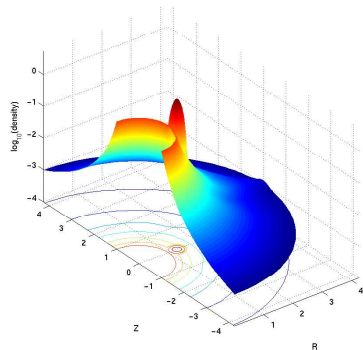
- fixed amount of flux:  
 $2\pi c_e \psi_0 \approx -6.6 \times 10^{20} \text{ Mx}$  in Northern hemisphere
- vary *flux emergence rate*, i.e.  $2\pi c_e \psi_0 / \Delta t$  from  $-3 \times 10^{18}$  to  $-5 \times 10^{16} \text{ Mx/s}$



Velocity of the flux rope center vs. time

## CME evolution: creating shocks

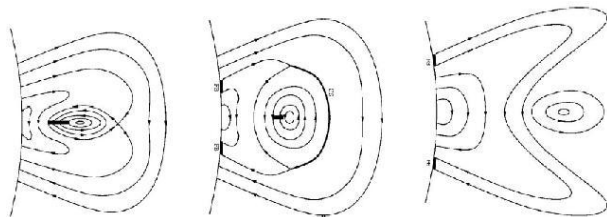
- Superpose a high-density & high-pressure plasma blob on the wind
- Initial perturbation of the density:  
 $\rho_{CME} = 5N_0$
- Initial perturbation of the velocity:  
 1000 km/s
- Plasma blob can contain a flux rope with same or opposite polarity of the background field



*Initial perturbation of the density*

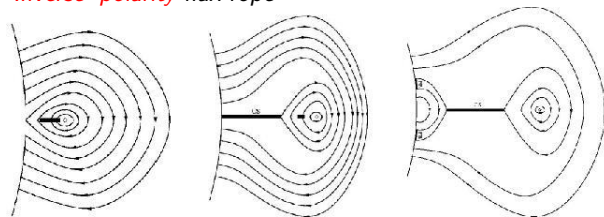
## CME evolution: Low & Zhang (2002) confirmed!

*'Normal' polarity flux rope*



## CME evolution: Low & Zhang (2002) confirmed!

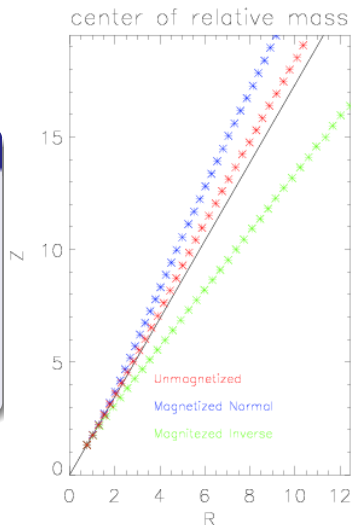
*'Inverse' polarity flux rope*



## Magnetic polarity of the flux rope

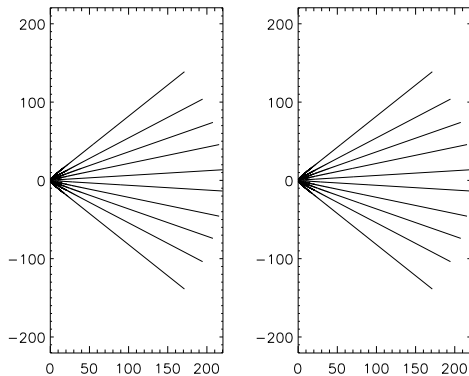
### Effect on evolution path...

- magnetic polarity of flux rope influences evolution path CME!
- effect has been quantified for different background wind models
- here only shown for Wind model 3 and initial launch angle 60 degrees



## CME evolution up to 1 AU

- self-similar evolution stops beyond  $30 R_{\odot}$
- difference normal/inverse polarity much smaller (e.g. density distr.)
- higher wind density at equator leads to serious deformation (compression) of the CMEs
- only difference :
  - about 6 hrs  $\neq$  in arrival time
  - orientation of field



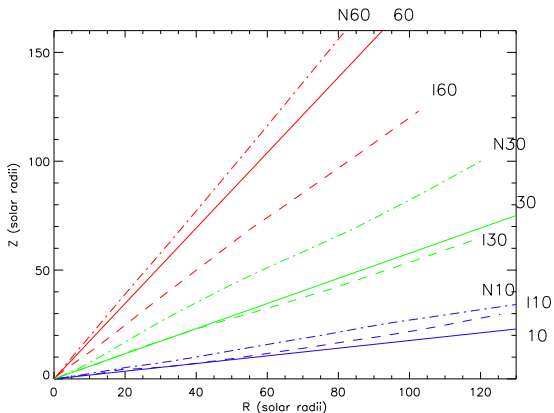
Relative density and magnetic field lines (INVERSE - NORMAL)



## Evolution path (Centre of Mass)

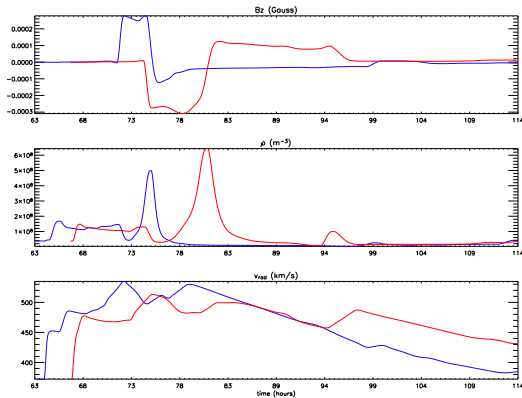
inverse CMEs still deviated towards equator but :

- difference smaller than at  $30 R_{\odot}$
- not true for  $\theta_{\text{CME}} \leq 10^{\circ}$  (due to high wind density at equator)



## Simulated satellite data at 1 AU (Wind model 2)

- Normal (blue) and inverse (red) CME
- 3-part structure of CME
  - 1 leading shock
  - 2 dark cavity
  - 3 high density core in cavity
- leading shock front
- . . .



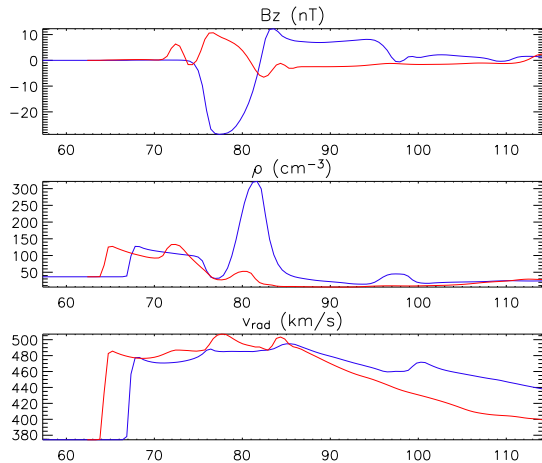
## Simulated satellite data at 1 AU (Wind model 2)

**effect of magnetic  
 polarity flux rope :**

for  $\theta_{\text{cme}} = 10^\circ$  :  
 magnetic cloud of

- normal CME misses
- inverse CME hits

the earth!

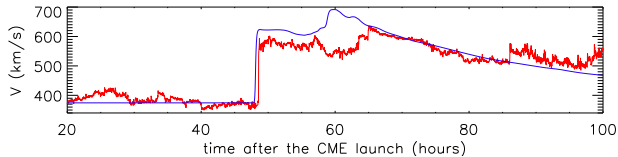
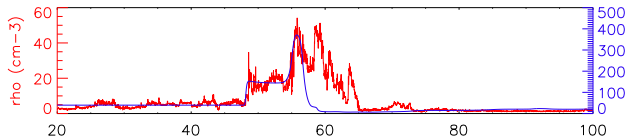
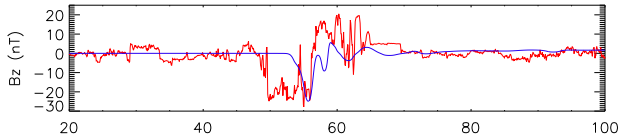


Inverse (blue) and normal (red) CME launched with  $\theta_{\text{cme}} = 10^\circ$

## Event study

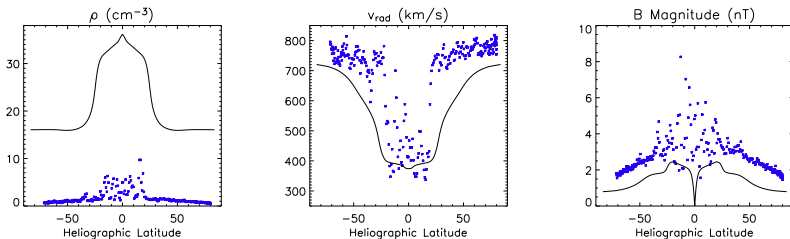
- full halo CME observed by LASCO and EIT on April 4, 2000
  - observed at 16:32 UT in C2 frame
  - related flare observed by EIT at 15:24 UT
  - C3 measurements : plane-of-the-sky speed is 984 km/s
- 
- try to match ACE data by
    - using wind model 2
    - playing with CME parameters ( $v_{\text{cme}}$ ,  $\theta_{\text{cme}}$ ,  $B_{\text{rope}}$ , polarity)

## Event study



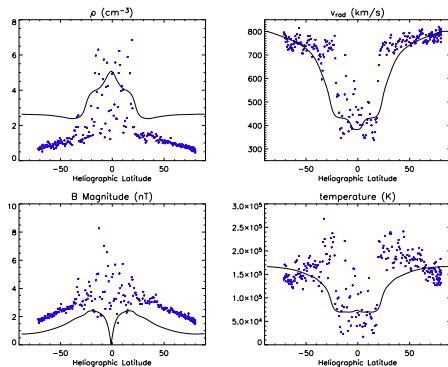
Best match :  
 inverse CME  
 with  $v_{\text{CME}} =$   
**1700 km/s**

However...



*Comparison of Ulysses data (between 1/11/94 and 1/08/95, i.e. when spacecraft was evolving between 1.34 and 2.03 AU) and wind model 2 at 1 AU*

## New wind model



*Comparison of Ulysses data (between 1/11/94 and 1/08/95, i.e. when spacecraft was evolving between 1.34 and 2.03 AU) and wind model 2 at 1 AU*

## Conclusions

The chosen **background wind model influences** :

- **the initiation of the CME (threshold, energetics, . . .)**
  - time of formation (threshold), energetics, speed, acceleration, . . .
- **evolution of the CME**
  - shape of leading shock front, shock speed, spread angle, mass distribution, . . .

Clearly, the **initial parameters** (shear velocity, polarity of fluxrope,  $v_{CME}$ ,  $\rho_{CME}$ ,  $\theta_{CME}$ , . . .) also influence the structure and evolution of the CME.